SenCom: Integrated Sensing and Communication with Practical WiFi

Yinghui He[1], Jianwei Liu[1], Mo Li[2,3], Guanding Yu[1,4], Jinsong Han[1,5], Kui Ren[1,5]

[1]Zhejiang University, Zhejiang, China.
[2]The Hong Kong University of Science and Technology, HongKong, China.
[3]Nanyang Technical University, Singapore.
[4]Jinhua Institute of Zhejiang University, Zhejiang, China.
[5]Key Laboratory of Blockchain and Cyberspace Governance of Zhejiang Province, Zhejiang, China.
{2014hyh,jianweiliu,yuguanding,hanjinsong,kuiren}@zju.edu.cn,lim@cse.ust.hk

ABSTRACT

Given the fact that WiFi-based sensing can be realized by reusing WiFi communication facilities and communication frequency bands, integrated sensing and communication (ISAC) is considered a crucial development direction for future WiFi standards, such as IEEE 802.11bf. Traditional WiFi sensing systems extract channel state information (CSI) from customized WiFi packets to quantify the characteristics of the sensing target. This poses challenges for existing WiFi systems originally designed for communication purposes, as it requires high-quality and sufficient CSI measurements. In this paper, we propose *SenCom*, which extracts CSI from general WiFi packets. *SenCom* enables CSI calibration across different WiFi communication modes and provides unified CSI measurements for upper-layer sensing applications. We also devise a fitting-resampling scheme to derive evenly sampled CSI with consistent dimensionality, and an incentive strategy to ensure sufficient CSI measurements over time. We build a prototype of *SenCom* and perform extensive experiments with 15 participants. The results show that *SenCom* is competent for a variety of sensing tasks, while incurring little compromise to the WiFi communication performance.

CCS CONCEPTS

• **Human-centered computing → Ubiquitous and mobile computing systems and tools**.

Yinghui He and Jianwei Liu contribute equally to this paper. Jinsong Han and Guanding Yu are the corresponding authors.

KEYWORDS

ISAC, WiFi, CSI

1 INTRODUCTION

Recent studies [35, 77, 82] demonstrate the non-intrusive sensing feasibility of a wide range of wireless radio frequency (RF) signals, among which WiFi is of special attraction due to its pervasive deployment [37]. Unfortunately, most existing WiFi sensing approaches are dependent on specific radio configurations and special purposed probing packets for detecting channel variations, which disrupts the normal WiFi function as a means of communication. In this paper, we explore a system solution to such a problem - enabling integrated sensing and communication (ISAC) [15, 53, 67] in practice without impairing the state-of-the-art communication routines of WiFi.

Instead of exploring extra spectrum usage or relying on exclusive transmissions for sensing, the proposed solution aims to make full use of the in-band WiFi communication traffic without introducing any extra overhead. Such a goal is hard to achieve because high-performance WiFi sensing requires quality and sufficiency in its channel state information (CSI), raising the following challenges. (i) Advanced WiFi (e.g., 802.11n/ac/ax [8]) supports multiple-input multiple-output (MIMO) communications [26], which alternates between different modes, i.e., diversity mode and multiplexing mode. These two modes possess different mapping matrices[1] for different numbers of data streams. The measured CSI cannot be directly translated to channel coefficients for sensing the object dynamics without knowing the specific MIMO setting. (ii) The beamforming [39] adopted in WiFi for strengthening

---

[1]The mapping matrix is also known as the precoding matrix.
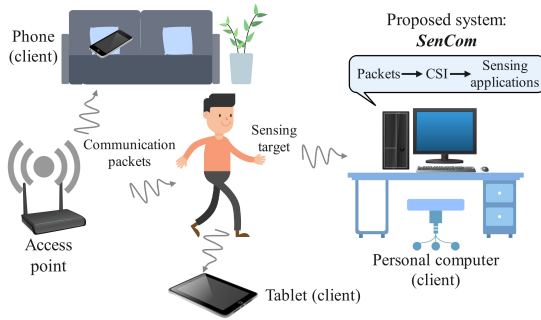
Figure 1: Application scenario of *SenCom*.

(a) Traditional WiFi sensing in communication environments.

(b) *SenCom*: Integrating sensing and communication.

Figure 2: Comparing traditional WiFi sensing with our ISAC solution-*SenCom*.

the signal directed to the communication clients may lead to weakened signals reflected from the sensing target, resulting in low sensing signal-to-noise ratio (SNR) that degrades the sensing performance. (iii) As general WiFi transmissions scatter unevenly in time due to varying communication demands, there may be insufficient packets to probe the channel at times, disabling the sensing.

In this paper, we address the above challenges and propose *SenCom*, to the best of our knowledge, the first practical ISAC system that enables seamless WiFi sensing with general communication traffic. Figure 1 depicts the *SenCom* usage scenario, where *SenCom* is implemented on one normal WiFi client and sniffs the ongoing WiFi transmissions between the WiFi AP and clients (including the client with *SenCom*). *SenCom* measures the CSI from the sniffed packets and derives the environment dynamics for various sensing tasks based on that. In such a way, there is no disruption to any of the ongoing WiFi communication flows between the AP and clients.

Specifically, we perform an in-depth analysis of different MIMO transmission modes and derive a transformation formula that transforms the CSI collected from various transmission modes into a unified form. Agnostic sensing applications can thus be performed with the unified CSI without knowing the configuration particulars of each WiFi transmission flow (which is WiFi AP/client-specific and often unknown to the sniffers). A compensation formula is derived to reconstruct the potential beamforming steering matrix and based on its inverse to suppress the impact of beamforming. In order to address uneven WiFi transmissions in time, we devise a fitting-resampling scheme to obtain CSI samples with consistent dimensionality, which benefits mapping and model training of upper-layer sensing applications. We further investigate the trade-off between the sensing and communication performance and inject active probing packets (i.e., incentive packets) with inadequate normal WiFi traffic, while minimizing its impact on the communication.

We implement a prototype of *SenCom* with commercial off-the-shelf (COTS) 802.11ac WiFi devices and conduct real-world experiments with 15 human participants in three different test environments. The experimental results show that
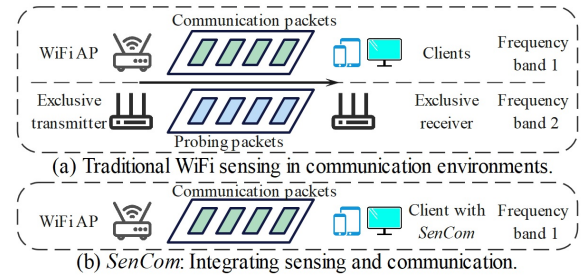
SenCom provides competent support to various sensing tasks with quality and sufficient CSI. After implementing *SenCom*, the throughput and delay of the communication system only drop by ~2%. Furthermore, reproducing two existing WiFi sensing applications demonstrates 94.4% accuracy for activity recognition and an error rate of 1.6% for step counting when applying *SenCom* to support ISAC.

In summary, our contributions are as follows: ❶ We propose *SenCom*, the first practical WiFi ISAC system that can be seamlessly integrated into existing communication systems to enable various sensing applications. *SenCom* can be implemented without modifying any existing WiFi communication standards, devices, or settings. ❷ To obtain qualified CSI and suppress the impact of conventional communication designs, *SenCom* embeds a CSI calibration method that includes a transformation formula to unify the CSI and a compensation formula to restrain the influence of beamforming. To obtain sufficient CSI, *SenCom* adopts a fitting-resampling scheme to support upper-layer sensing applications, as well as an incentive strategy to elicit compensation probing packets where a closed-form incentive rate is derived to balance sensing and communication performance. ❸ We build a prototype of *SenCom* and conduct real-world experiments on it. The experimental results demonstrate that *SenCom* significantly improves the quantity and quality of the CSI collected in a communication context, while hardly impacting the communication throughput and latency. Case studies on real sensing applications show that *SenCom* performs well in various sensing tasks.

2 BACKGROUND AND PROBLEM STATEMENT

2.1 Traditional WiFi Sensing

WiFi sensing has been extensively studied for many years. A conventional WiFi sensing system employs a pair of transceivers to probe environmental changes, as shown in Fig. 2(a). This is an active sensing manner, where the transmitter only transmits pre-designed probing packets to the receiver at a constant transmission rate. The entire sensing system is isolated from the communication function. To
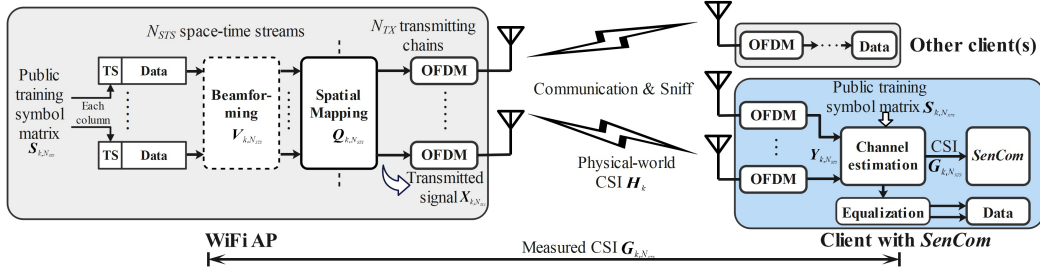
Figure 3: Signal transmission procedure. 'TS' represents the training symbol vector.

implement the sensing system in an environment, two *additional* and *exclusive* transceivers must be deployed as the transmitter and receiver, respectively. To avoid impacting the communication system already present in this environment, the sensing system must use an *extra* frequency band that is different from the communication system. As a result, the implementation of a traditional WiFi sensing system not only incurs large hardware overhead but also wastes spectrum resources.

In contrast, *SenCom* combines both passive and active sensing techniques. The former enables *SenCom* to sniff and make full use of the off-the-shelf packets from existing communication systems (e.g., WiFi APs), while the latter helps *SenCom* obtain sufficient sensing information. As shown in Fig.2(b), our approach *does not introduce any extra hardware overhead*. Furthermore, since the sensing channel and the communication channel share the same frequency band, *SenCom* also *halves the consumption of spectrum resources* compared to the traditional solution.

2.2 Problem and Challenge

In this part, we explain the challenges in achieving our proposal, ISAC, in a practical communication context. We start by reviewing the data transmission procedure of the 802.11ac Wave 1 standard [6], which has been widely adopted in existing WiFi systems. This procedure utilizes the MIMO technique to enable simultaneous transmissions of multiple data streams (i.e., space-time streams (STSs) [6]) between the WiFi AP and the client via multiple antennas[2], as shown in Fig. 3. To eliminate the unknown channel effect and ensure correct decoding at the client, each data stream transmitted from the AP has its own training symbol vector, which is utilized for measuring CSI and channel equalization. All training symbol vectors of N_{STS} STSs make up a training symbol matrix. *Sen-Com* passively measures the CSI based on the sniffed training symbol matrix. Specifically, before being transmitted by the antennas, the training symbol matrix needs to go through three main processes. (i) Potentially, for beamforming and directional transmission, the training symbol matrix first passes the steering matrix. (ii) The number of data streams may be unequal to that of transmitting antennas. Thus, a

---

[2]We use data stream and STS interchangeably throughout the paper.

mapping matrix is needed for mapping the N_{STS} data streams to N_{TX} transmitting chains for subsequent transmission. (iii) To avoid inter-code interference, orthogonal frequency division multiplexing (OFDM) modulation [68] divides wireless bandwidth into K subcarriers for parallel transmission. Let $\mathbf{S}_{k,N_{STS}} \in \mathbb{C}^{N_{STS} \times N_{STS}}$ denote the training symbol matrix of N_{STS} STSs for subcarrier k, where each row of $\mathbf{S}_{k,N_{STS}}$ corresponds to the training symbol vector for each data stream and $\mathbb{C}$ is the set of complex numbers. The final transmitted signal at the WiFi AP for subcarrier k can be expressed by:

$$\mathbf{X}_{k,N_{STS}} = \mathbf{Q}_{k,N_{STS}} \mathbf{V}_{k,N_{STS}} \mathbf{S}_{k,N_{STS}}, \tag{1}$$

where $\mathbf{Q}_{k,N_{STS}} \in \mathbb{C}^{N_{TX} \times N_{STS}}$ represents the mapping matrix and $\mathbf{V}_{k,N_{STS}} \in \mathbb{C}^{N_{STS} \times N_{STS}}$ denotes the steering matrix for potential beamforming. When $N_{STS} = 1$, the transmitter works in the diversity mode; otherwise, the transmitter works in the multiplexing mode.

After undergoing the physical-world wireless channel, denoted by $\mathbf{H}_k \in \mathbb{C}^{N_{RX} \times N_{TX}}$ for subcarrier k, and OFDM demodulation, the signal sniffed at *SenCom* is:

$$\mathbf{Y}_k = \mathbf{H}_k \mathbf{X}_{k,N_{STS}} + \mathbf{N}_0 = \mathbf{H}_k \mathbf{Q}_{k,N_{STS}} \mathbf{V}_{k,N_{STS}} \mathbf{S}_{k,N_{STS}} + \mathbf{N}_0, \tag{2}$$

where $\mathbf{N}_0 \in \mathbb{C}^{N_{RX} \times N_{STS}}$ is the Gaussian white noise with N_{RX} being the number of the receiving antennas. As shown in Fig. 3, *SenCom* uses the public training symbol matrix to measure CSI from $\mathbf{Y}_k$. As *SenCom* is not aware of the configurations of transmitting antennas at the AP side, in its view, the received signal at each receiving antenna is a superimposed signal as if it came through a steered wireless channel from a "virtual antenna". The CSI measured at *SenCom* can thus be expressed as:

$$\mathbf{G}_{k,N_{STS}} = \mathbf{H}_k \mathbf{Q}_{k,N_{STS}} \mathbf{V}_{k,N_{STS}}. \tag{3}$$

$\mathbf{G}_{k,N_{STS}}$ describes the channel between the virtual antennas and receiving antennas at *SenCom*, and is affected by the MIMO and beamforming techniques. Therefore, it is different from the physical-world CSI $\mathbf{H}_k$ that describes the channel between the transmitting antennas and receiving antennas. **Challenge 1-Qualified CSI.** As *SenCom* passively sniffs the WiFi traffic between the AP and clients, it has no knowledge of the MIMO and beamforming configurations used on the AP side. This raises two problems. First, the AP could operate in either the diversity or multiplexing mode based on the
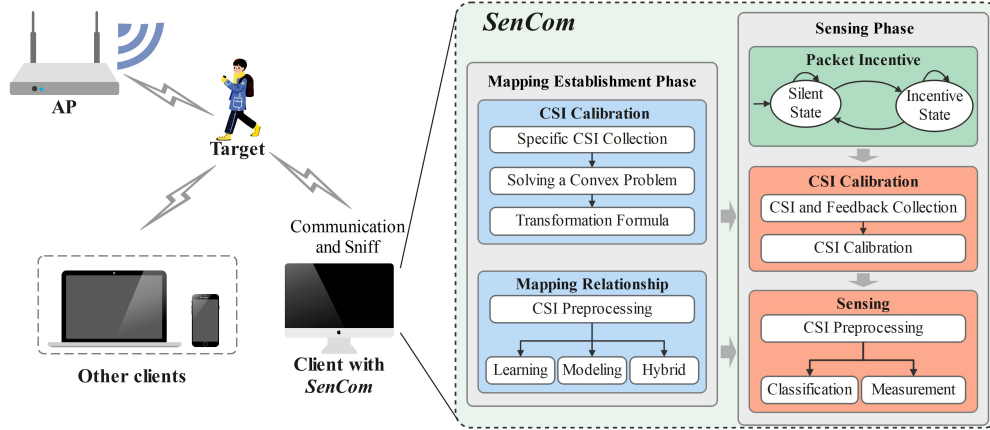
Figure 4: Architecture of *SenCom*.

client's demands, and this mode switch is unpredictable for a passive monitor like *SenCom*. Thus, *SenCom* does not know which mode the AP is working in. Unfortunately, the CSI collected under different modes is different even though the real environment does not change (based on Eq. 3), resulting in that the sensing model established in one mode cannot perform adequately in another. *So, the sensing model of which mode should be used is agnostic to SenCom.* On the other hand, the beamforming leads to directional transmission, which may *weaken the signal towards the sensing target and thus impair the SNR of the collected CSI* in deriving accurate sensing results. *SenCom* has to compensate for such an effect in its design.

Challenge 2-Sufficient CSI. WiFi sensing necessitates a sufficient amount of CSI related to the sensing target. Traditional WiFi sensing systems achieve this by configuring the AP to send probing packets at even and short time intervals [82] (usually less than 20 ms). In the considered ISAC practice, however, the transmitter (e.g., AP) sends data packets based only on the communication needs of the connected clients. The clients may require only intermittent downlink traffic, which is unevenly distributed and may be inadequate from time to time. Meanwhile, sensing only depends on beacon packets is impractical as the interval between beacon packets is typically set to 100 ms in existing WiFi systems, which is too large to support many sensing applications. *SenCom* has to adapt to practical WiFi systems, transform the sampled CSI into the evenly-distributed one, and trigger extra probing packets when necessary.

3 SYSTEM OVERVIEW

As shown in Fig. 4, *SenCom* collects CSI of the wireless channel from the AP by sniffing its transmissions to various clients. The operation of *SenCom* is composed of two primary phases: *mapping establishment phase* and *sensing phase*.

In *mapping establishment phase*, *SenCom* performs pre-calibration for CSI and establishes a mapping relationship between the CSI and sensing objective. Specifically, in CSI calibration, *SenCom* needs to collect the CSI of two modes by accessing the AP. Then, based on the collected CSI, a key transformation matrix for unifying CSI is figured out. Afterwards, *SenCom* performs a series of potential preprocessing like fitting-resampling on the calibrated CSI to support upper-layer applications. An application can be realized by establishing a mapping relationship (modeling-based, learning-based, or hybrid [53]) between the CSI and the sensing objective.

In *sensing phase*, *SenCom* performs sensing tasks with the pre-established mapping relationship, during which our incentive strategy keeps running to guarantee sufficient CSI. Specifically, *SenCom* first collects the CSI samples and the feedback on beamforming of the clients. With the pre-acquired transformation formula and a compensation formula for suppressing the impact of beamforming, the collected CSI samples can be calibrated into a unified form. The same preprocessing techniques used in the *mapping establishment phase* are then applied to the CSI samples. Since WiFi-based sensing is either classification-driven or measurement-driven [53], the pre-processed CSI will be fed into the mapping relationship to perform classification or measurement tasks.

4 CSI CALIBRATION

This section presents a CSI calibration method aimed at mitigating the negative effects of particular communication designs, such as MIMO and beamforming, on the sensing performance.

4.1 CSI Transformation

Having multiple transmitting antennas allows the AP to use either the diversity mode or multiplexing mode to achieve
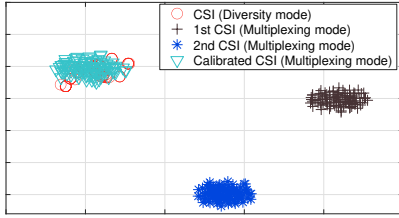
Figure 5: CSI distribution under diversity mode is different from that under multiplexing mode. Our calibration method can unify the CSI distribution.

specific communication purposes. This brings the first challenge introduced in Section 1. In this part, we first review the equation of CSI in Eq. 3 to figure out why this challenge arises. Without loss of generality, to make it easier to understand, we take a two-antenna AP as an example and consider that *SenCom* has one receiving antenna. Then, we introduce the difference between the CSI of the two modes and show how to transform the CSI of the multiplexing mode to that of the diversity mode. Note that we do not consider the beamforming here and leave it to the next part.

4.1.1 CSI Discrepancy Between Two Modes. In the diversity mode, there is only one data stream ($N_{STS} = 1$). It happens when the client has only one antenna or the client needs stability instead of high throughput. Only one training symbol s_k is allocated to the data stream for subcarrier k, that is, $\mathbf{S}_{k,N_{STS}}$ in Fig. 3 becomes s_k when $N_{STS} = 1$. Then, the training symbol is mapped into two transmitting chains with a mapping matrix $\mathbf{Q}_{k,1} = [q_{k,1}, q_{k,2}]^T$. The symbols in these two transmitting chains are $x_{k,1} = q_{k,1}s_k$ and $x_{k,2} = q_{k,2}s_k$, respectively. After going through the wireless channel $\mathbf{h}_k = [h_{k,1}, h_{k,2}]$ between the AP and *SenCom*, the received signal at *SenCom* is y_k. In this case, *SenCom* can only 'see' one virtual transmitting antenna instead of two real ones, because the AP only sends one training symbol and the signals from two real transmitting antennas are superimposed. The measured CSI between the virtual transmitting antenna and the receiving antenna is:

$$g_{k,1} = \mathbf{h}_k \mathbf{Q}_{k,1}. \tag{4}$$

In this mode, the physical-world CSI $\mathbf{h}_k$ between the AP and *SenCom* is transformed into $g_{k,1}$.

In the multiplexing mode, the transmitting process is similar to that in the diversity mode. *The differences lie in the training symbol and mapping matrix.* Two training symbol vectors are used in the multiplexing mode instead of one training symbol. Meanwhile, the mapping matrix used in the diversity mode is $\mathbf{Q}_{k,1} = [q_{k,1}, q_{k,2}]^T$, but what used in the multiplexing mode becomes:

$$\mathbf{Q}_{k,2} = \begin{bmatrix} q_{k,1,1} & q_{k,1,2} \\ q_{k,2,1} & q_{k,2,2} \end{bmatrix}.$$

Thus, in the multiplexing mode, after undergoing the wireless channel, *SenCom* can 'see' two virtual transmitting antennas. The measured CSI between the virtual transmitting antennas and the receiving antenna is:

$$\mathbf{g}_{k,2} = \mathbf{h}_k \mathbf{Q}_{k,2}. \tag{5}$$

Conclusion: From Eq. 4 and 5, we can find that the CSI collected under different modes can vary even when the environment remains unchanged. Particularly, we can get one CSI stream in the diversity mode but two in the multiplexing mode. To illustrate such differences, we collect two batches of CSI samples under these two modes in a static environment and reduce CSI's dimensionality with t-SNE algorithm [69]. The resulting CSI distributions are shown in Fig. 5. It can be seen that the CSI of the diversity mode is far from that of the multiplexing mode. Meanwhile, the two CSI streams of the multiplexing mode also scatter in different clusters. These two modes demonstrate three distinct CSI distributions, making it challenging to establish a mapping relationship that works well in both modes. A straightforward solution is to respectively establish three different mapping relationships for the two modes, allowing *SenCom* to choose the most suitable one according to the AP's working mode. However, it would require direct communication and coordination between *SenCom* and the AP, which would undermine our goal of achieving sensing without compromising communication performance.

4.1.2 CSI Transformation From Multiplexing to Diversity. To achieve accurate sensing without comprising the communication performance, we seek to unify the CSI of the two modes into a single distribution, such that only one mapping relationship is needed for sensing. For doing so, there are two potential ways: i) Both extracting physical-world CSI from the diversity mode and multiplexing mode. ii) Transforming the CSI of the multiplexing mode into that of the diversity mode. However, in the diversity mode, the physical world CSI $\mathbf{h}_k$ cannot be recovered from $g_{k,1}$ via Eq. 4, as there are infinite possible combinations for $\mathbf{h}_k$. Thus, *CSI transformation from the multiplexing mode to the diversity mode is the sole solution.*

Such a transformation can be achieved in two steps: (i) recovering the physical-world CSI from the multiplexing mode by multiplying $\mathbf{Q}_{k,2}^{-1}$ in both sides of Eq. 5; (ii) transforming the recovered CSI into the diversity mode using Eq. 4. We can derive the transformation formula as:

$$g_{k,1} = \mathbf{g}_{k,2} \mathbf{P}_k, \tag{6}$$

where $\mathbf{P}_k \triangleq \mathbf{Q}_{k,2}^{-1} \mathbf{Q}_{k,1}$ is the transformation matrix from the multiplexing mode to the diversity mode.

Now, the challenge turns into how to get $\mathbf{P}_k$. In fact, $\mathbf{P}_k$ is unknown to *SenCom* and it cannot be obtained through simple theoretical derivations. To address this issue, we heuristically take advantage of real CSI and propose an optimization-based approach to estimate $\mathbf{P}_k$. To be specific, we first noticed that the CSI is invariable during the coherence time [76]. Under this property, as long as in the coherence time, the CSI collected in the diversity mode is consistent with that collected in the multiplexing mode. It is potential to leverage such consistency to estimate $\mathbf{P}_k$. In particular, we place a two-antenna client (e.g., phone) and *SenCom* near the AP to access and 'ping' the AP in the coherence time, respectively. Since the AP works in the multiplexing/diversity mode when communicating with the client/*SenCom*, we can collect CSI samples of the two modes. To further make the estimated $\mathbf{P}_k$ more accurate, we can collect several groups of CSI samples in different environments. Let $\left\{g_{k,1}^{(i,1)}, \mathbf{g}_{k,2}^{(i,2)}\right\}$ and I denote the i-th CSI sample pair and the number of pairs, respectively. Thanks to CSI's invariability in the coherence time, $\mathbf{g}_{k,2}^{(i,2)}\mathbf{P}_k$ (from the multiplexing mode) is equal to $g_{k,1}^{(i,1)}$ (from the diversity mode) in theory, so that we can calculate $\mathbf{P}_k$ with the least squares optimization problem:

$$\min_{\mathbf{P}_k} \ \Sigma_i \left\| g_{k,1}^{(i,1)} - \mathbf{g}_{k,2}^{(i,2)}\mathbf{P}_k \right\|^2.$$

Nonetheless, due to the phase error $\Delta\gamma_i$ brought by the receiver of *SenCom* and varied channel gain, $g_{k,1}^{(i,1)}$, and $\mathbf{g}_{k,2}^{(i,2)}\mathbf{P}_k$ are not exactly the same in practice. Based on the previous study [75], phase variation between two CSI samples during the coherence time is caused by the packet boundary detection uncertainty and $\Delta\gamma_i$ follows a Gaussian distribution with zero mean. Taking into account the phase error and varied channel gain, we have the following relationship between the CSI samples of the two modes: $\alpha_i g_{k,1}^{(i,1)} = \mathbf{g}_{k,2}^{(i,2)}\mathbf{P}_k$, where $\alpha_i = |\alpha_i|e^{j\Delta\gamma_i}$ and $|\alpha_i|$ describes the variation of channel gain with $\mathbb{E}\left\{|\alpha_i|^2\right\} = 1$. $\mathbf{P}_k$ can be estimated by $\min_{\alpha_i, \mathbf{P}_k} \ \Sigma_i \left\| \alpha_i g_{k,1}^{(i,1)} - \mathbf{g}_{k,2}^{(i,2)}\mathbf{P}_k \right\|^2$. Thereafter, we introduce a fractional form to prevent α_i and $\mathbf{P}_k$ from being zero. The optimization problem can be rewritten as:

$$\min_{\hat{\alpha}_i, \hat{\mathbf{P}}_k} \ \sum_i \left\| \hat{\alpha}_i g_{k,1}^{(i,1)} - \mathbf{g}_{k,2}^{(i,2)}\hat{\mathbf{P}}_k \right\|^2, \ \text{s.t. } \hat{\mathbf{P}}_k(1,1) = 1, \quad (7a)$$

which is convex since it is a quadratic optimization problem and can be solved with existing solvers, such as CVX [23].

After obtaining the optimal solution to the problem in Eq. 7, we need to obtain $P_k(1,1)$ for calculating $\mathbf{P}_k$. Recalling that the channel gain variation follows $\mathbb{E}\left\{|\alpha_i|^2\right\} = 1$, we can estimate $P_k(1,1)$ as:

$$P_k(1,1) = \sqrt{\frac{1}{I} \sum_{i=1}^{I} |\hat{\alpha}_i|^2} e^{-j\frac{1}{I}\sum_{i=1}^{I} \angle\hat{\alpha}_i}, \quad (8)$$
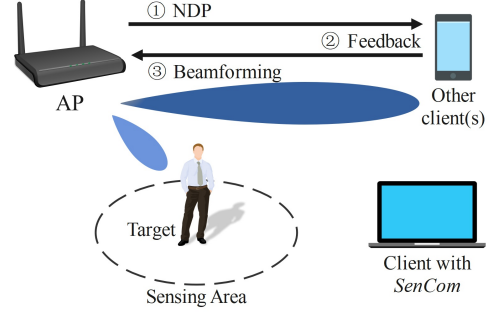
Figure 6: Transmission procedure with beamforming.

where $\angle\hat{\alpha}_i$ represents the phase of $\hat{\alpha}_i$. Ultimately, the transformation matrix $\mathbf{P}_k$ can be estimated by $\mathbf{P}_k = P_k(1,1)\hat{\mathbf{P}}_k$. In this way, all the collected CSI can be unified into one mode/distribution using estimated $\mathbf{P}_k$. As shown in Fig. 5, the CSI transformed from the multiplexing mode and that of the diversity mode lies in the same cluster. This demonstrates that they have the same distribution and our transformation is very effective. *Note that, since $Q_{k,1}$ and $Q_{k,2}$ are independent of the wireless channel and only related to the AP, the transformation matrix $\mathbf{P}_k$ only depends on the AP also. Therefore, $\mathbf{P}_k$ can be permanently used across time and environments once it was estimated.*

4.2 Compensation for Beamforming

Principle of beamforming. This part focuses on beamforming, which is utilized in WiFi 802.11ac/ax to enhance communication throughput. Figure 6 depicts The transmission procedure with beamforming, where the AP sends a null data packet (NDP) to the client prior to data transmission. The client measures the CSI, denoted by $\mathbf{H}_k^c$ for subcarrier k, and feeds it back to the AP.[3] The AP utilizes the received feedback to create a steering matrix $\mathbf{V}_{k,N_{STS}}$ to facilitate the directional transmission towards the client. *However, from the perspective of SenCom, the power of the signal passing through the sensing area may become much weaker than that of other areas, leading to a reduction in the SNR of the CSI.* Thus, we need to suppress the impact of beamforming in the following.

Suppressing the impact of beamforming. According to Eq. 3, we need to eliminate the steering matrix $\mathbf{V}_{k,N_{STS}}$ in the collected CSI by the following compensation formula:

$$\mathbf{G}_{k,N_{STS}}\mathbf{V}_{k,N_{STS}}^{-1} = \mathbf{H}_k\mathbf{Q}_{k,N_{STS}}. \quad (9)$$

---

[3]Here, we mainly consider the cases where the sniffed packets are from the clients without implementing *SenCom*, as the obtained $\mathbf{H}_k^c$ does not describe the real channel between the AP and *SenCom*. If the sniffed packets are from the client that *SenCom* is implemented on, the obtained $\mathbf{H}_k^c$ can be directly used for sensing and there is no need to listen to the feedback of NDP.

We cannot directly apply this formula because the steering matrix $\mathbf{V}_{k,N_{STS}}$ is unknown to a passive monitor like *Sen-Com*. Fortunately, *SenCom* can listen to the feedback of NDP, i.e., $\mathbf{H}_k^c$, as it is used for creating $\mathbf{V}_{k,N_{STS}}$. Without loss of generality, $\mathbf{V}_{k,N_{STS}}$ can be derived from $\mathbf{H}_k^c$ suppose that we know the structuring method of the adopted beamforming scheme. Here, we assume that the AP adopts zero-forcing (ZF) beamforming [80], as it is one of the most popular ones [58]. Then, after sniffing the CSI measured by the client (i.e., $\mathbf{H}_k^c$), the steering matrix can be calculated at *SenCom* by: $\mathbf{V}_{k,N_{STS}} = ((\mathbf{H}_k^c)^H \mathbf{H}_k^c)^{-1} (\mathbf{H}_k^c)^H$, where $(\cdot)^H$ is the operation of conjugate transpose. With the calculated $\mathbf{V}_{k,N_{STS}}$, *SenCom* can effectively suppress the impact of beamforming with the compensation formula (Eq. 9). Under the premise that *SenCom* has the knowledge of the beamforming strategy employed by the AP, the above compensation method can be easily extended to other beamforming schemes by simply replacing the steering matrix. For example, for the singular value decomposition (SVD) beamforming [68], the steering matrix can be given by $\mathbf{V}_k$ with the SVD of the CSI measured by the client (i.e., $\mathbf{H}_k^c$) being $\mathbf{H}_k^c = \mathbf{U}_k \mathbf{\Sigma}_k \mathbf{V}_k$.

5 UNIFYING CSI SAMPLING

In traditional WiFi sensing (Sec. 2.1), packets are transmitted at a consistent and evenly-spaced interval, ensuring that the sampled CSI's dimensionality is consistent for upper-layer sensing applications. But it is hard to guarantee such evenness in communication traffic with varying downlink data demands. To overcome this problem, we devise a fitting-resampling scheme to maintain the uniformity of CSI scatters in the time domain. In cases the normal communication packets are insufficient, we suggest an incentive strategy to encourage the AP to send compensation packets. In its design, we model the trade-off between the sensing and communication performance, ensuring that *SenCom* can obtain adequate packets without significantly degrading the communication channel.

5.1 Fitting and Resampling

When clients require high communication demands, *SenCom* can obtain sufficient packets for sensing. However, since the communication packets are not evenly distributed over time, the number of packets collected in a fixed-length time period is variable. This variability makes it difficult to ensure that input CSI samples have consistent dimensionality, which is crucial for upper-layer applications of many sensing systems, especially those employing learning models. For example, in a WiFi-based sign language recognition system SignFi [54], the default dimensionality of the CSI amplitude fed into the convolutional neural network is fixed as (3, 30, 200), where 3×30 is the number of subcarriers and the last dimension

(a) CSI amplitude variation traces of four subcarriers.

(b) Fitted CSI amplitude curves of four subcarriers.

(c) CSI phase variation traces of four subcarriers.

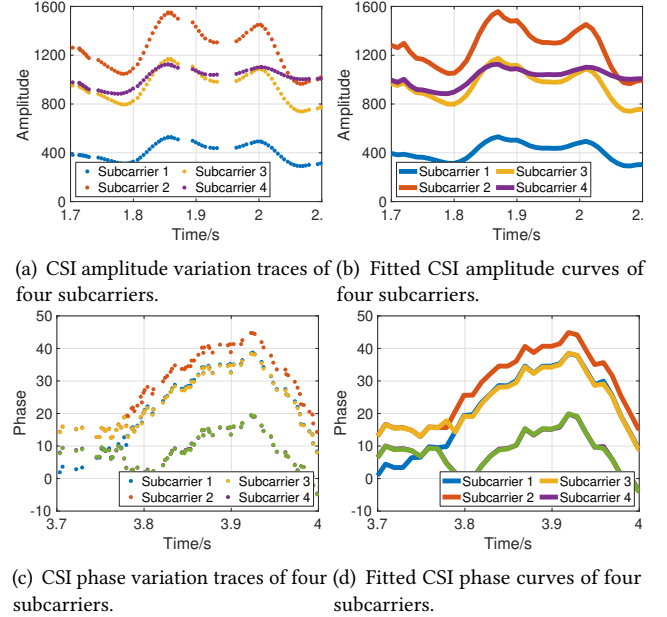(d) Fitted CSI phase curves of four subcarriers.

Figure 7: Cubic spline fitting results.

means evenly collecting 200 packets for each CSI sample. For this purpose, we propose to fit the variation trace of each subcarrier in the CSI sample, and then resample the fitted function at an equal interval. Specifically, we opt to perform cubic spline fitting [10], because we observed that the variation trace of each subcarrier is akin to the splicing of multiple cubic functions in the time domain (i.e., cubic function in each small time window). The objective of cubic splines is to derive a third-order polynomial for each CSI interval, which can be formulated as $f_i(t) = a_i t^3 + b_i t^2 + c_i t + d_i$, where t is timestamp, and i means the i_{th} CSI interval. a_i, b_i, c_i, and d_i are four parameters that require evaluation. The fitting results of four subcarriers are shown in Fig. 7. It can be observed that the fitted curves (Figs. 7(b) and 7(d)) closely resemble the real variation traces of the subcarriers (Figs. 7(a) and 7(c)). Therefore, cubic spline curves can precisely fit the sensing information recorded by CSI. After that, we sample at an equal interval on spline functions. In this way, *SenCom* is able to maintain a stable sampling rate to provide dimensionality-consistent CSI samples for upper-layer applications.

5.2 Incentive Strategy

In situations where clients have no communication demands, there is no ongoing packet for *SenCom* to sample the CSI. To address this issue, we design an incentive strategy based on queuing theory [63]. This strategy enables *SenCom* to alternate between two states to obtain sufficient incentive packets (i.e., probing packets), while hardly compromising the communication performance.

State definition. We assume that the arrival process of communication packets at the AP follows the Poisson process[4] with a rate $\lambda^c[t]$[5] (in packets/s) at time index t. Let F^{re} (in packets/s) denote the required sensing frequency, i.e., the required CSI sampling rate. By comparing F^{re} with $\lambda^c[t]$, we have the following two states in the incentive strategy. (i) *Silent state*: it refers to the state when $\lambda^c[t] \geq F^{re}$. In this state, the AP does not need to transmit incentive packets and *SenCom* only estimates CSI from communication packets. (ii) *Incentive state*: it refers to the state when $\lambda^c[t] < F^{re}$. In this state, *SenCom* drives the AP to transmit incentive packets with an incentive rate $\lambda^i[t]$ and collects CSI simultaneously.

Incorporating communication loss. Next, we only need to consider the performance in the incentive state as transmitting incentive packets may affect the communication performance. We do not want to impair any ongoing communication traffic when injecting extra probing packets during the incentive state. To be specific, the *sensing performance* can be described with the CSI sampling rate, i.e., $\lambda^c[t] + \lambda^i[t]$, and the communication performance can be analyzed with queueing theory. The communication latency without incentive packets is given by:

$$\tau^c[t] = \frac{\lambda^c[t]\mathbb{E}\left\{W^2\right\}}{2\left(1 - \lambda^c[t]\mathbb{E}\left\{W\right\}\right)} + \mathbb{E}\left\{W\right\}, \qquad (10)$$

where W is the transmission latency and $\mathbb{E}\left\{\cdot\right\}$ is the operation of expectation. With $\lambda^c[t]\mathbb{E}\left\{W\right\} < 1$, every packet is delivered successfully and the corresponding throughput is the product of the rate $\lambda^c[t]$ and the data size per packet. By contrast, with incentive packets, the communication latency becomes:

$$\tau^{c,i}[t] = \frac{\left(\lambda^c[t] + \lambda^i[t]\right)\mathbb{E}\left\{W^2\right\}}{2\left(1 - \left(\lambda^c[t] + \lambda^i[t]\right)\mathbb{E}\left\{W\right\}\right)} + \mathbb{E}\left\{W\right\}. \qquad (11)$$

Moreover, when $\left(\lambda^c[t] + \lambda^i[t]\right)\mathbb{E}\left\{W\right\} < 1$, the throughput keeps unchanged. Therefore, we only consider the *latency loss*, as $\Delta\tau[t] = \tau^{c,i}[t] - \tau^c[t]$.

Balancing sensing and communication. To enable sensing without hurting communication, we formulate the following optimization problem:

$$\max_{\lambda^i[t]} \quad \beta\left(\lambda^c[t] + \lambda^i[t]\right) - (1-\beta)\Delta\tau[t], \qquad (12a)$$

$$\text{s.t.} \quad \left(\lambda^c[t] + \lambda^i[t]\right)\mathbb{E}\left\{W\right\} \leq 1 - \epsilon, \qquad (12b)$$

$$\lambda^i[t] \geq 0, \qquad (12c)$$

where β denotes the weight and $\epsilon > 0$ denotes the tolerance. The objective function in Eq. 12a describes the trade-off between sensing performance and communication latency.

[4]In practice, most of the communication traffic follows the Poisson process [19].

[5]$\lambda^c[t]$ can be obtained by the forecasting method, such as the time series model and long short-term memory (LSTM) [16].
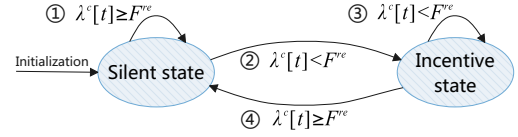
Figure 8: Incentive strategy.

The constraint in Eq. 12b ensures that the communication throughput is not affected by the incentive packets. It is easy to prove the convexity of the above problem and the corresponding optimal solution is given by:

$$\lambda^{i,\star}[t] = \left[\frac{1}{\mathbb{E}\left\{W\right\}}\left(1 - \sqrt{\frac{1-\beta}{2\beta}\mathbb{E}\left\{W^2\right\}}\right) - \lambda^c[t]\right]_0^{\frac{1-\epsilon}{\mathbb{E}\{W\} - \lambda^c[t]}}, \quad (13)$$

where $[x]_A^B = \min\{B, \max\{x, A\}\}$. From Eq. 13, we can find that the incentive rate $\lambda^i[t]$ is affected by β. If we prefer better sensing performance than less communication loss, we can empirically set a high β to get a large incentive rate.

Overall view. The optimal incentive rate in the incentive state is now clear. As shown in Fig. 8. The incentive strategy contains two states, and the transition conditions between the two states are determined by the arrival rate of communication packets $\lambda^c[t]$ and the required sensing frequency F^{re}. If $\lambda^c[t] \geq F^{re}$, the next state is the silent state; otherwise, the next state is the incentive state. In the silent state, *SenCom* collects CSI by listening to communication packets. In the incentive state, *SenCom* drives the AP to transmit incentive packets with rate $\lambda^i[t]$ given in Eq. 13. This design effectively address the issue of CSI insufficiency while keeping communication loss very low.
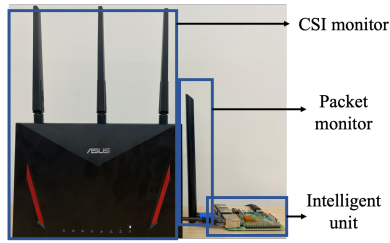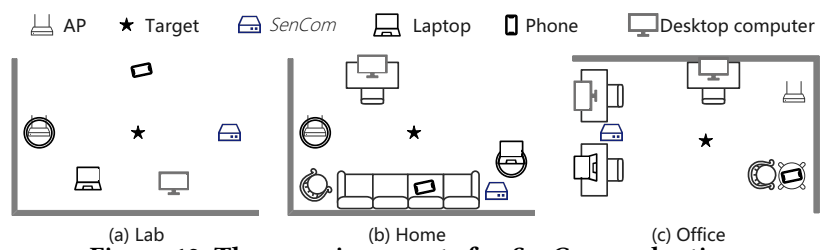
6 EVALUATION

This section presents the real-world implementation and details the performance of *SenCom* in terms of sensing and communication.

6.1 Implementation

As shown in Fig. 9, we implement *SenCom* on a standalone sensing client comprising a CSI monitor, a packet monitor, and an intelligent unit. Not using an off-the-shelf client to embark *SenCom* is indeed an engineering compromise. Even though most existing WiFi network interface cards (NICs) on the clients are able to sniff packets and measure the CSI, the NIC manufacturers do not provide corresponding permissions as these abilities are useless for upper-layer non-sensing applications. Nonetheless, it is noteworthy that NICs are technically capable of performing all the functions required by *SenCom*, and it is technically trivial to modify *SenCom* to work with a single WiFi NIC should the CSI information is internally accessible from the NIC. We believe that our work will encourage manufacturers to open the interfaces for these abilities. In our *SenCom* prototype, the

Figure 9: Prototype of *SenCom*.

(a) Lab   (b) Home   (c) Office

Figure 10: Three environments for *SenCom* evaluation.

CSI monitor measures CSI from received packets, while the packet monitor is responsible for receiving the feedback of beamforming. The intelligent unit wirelessly connects to an AP and performs incentive strategy, CSI calibration, fitting, resampling, and finally gets the sensing result. More specifically, we implement *SenCom* on a Raspberry Pi 4B connected to a TP-LINK WDN5200H (a Wireless USB WiFi Adapter) and an ASUS RT-AC86U Router. The Raspberry Pi 4B works as the intelligent unit, and the TP-LINK WDN5200H is configured in the monitor mode working as the packet monitor. The ASUS RT-AC86U Router installed with the Nexmon CSI tool [24] is used as the CSI monitor. Note that we have modified Nexmon CSI tool so that it can distinguish whether beamforming is utilized in the packet while logging CSI from the received packet.

We conduct experiments in three different environments, including a lab, a home, and an office, as shown in Fig. 10. To mimic a real communication scenario, a Mi Router Mini[6] and three clients are included. The router works as an AP with a bandwidth of 20 MHz. The clients include a laptop with a one-antenna wireless adapter (TP-LINK WDN5200H), a phone (Google Pixel 4) with two antennas, and a desktop computer with a three-antenna network interface card (TP-LINK TL-WDN7280). In our default communication context, the Google Pixel 4 phone is connected to the AP and plays online videos.

We focus on the standard of 802.11ac Wave 1 since it is one of the most pervasive WiFi standards in existing WiFi devices. In this standard, OFDM, MIMO, packet aggregation, beamforming, and other techniques are adopted to enhance channel efficiency. Our work can also be easily extended to the subsequent WiFi standards, i.e., 802.11ac Wave 2 and 802.11ax, where orthogonal frequency division multiple access (OFDMA) and multi-user multiple-input multiple-output (MU-MIMO) are adopted for high communication performance. With the OFDMA, the AP can allocate different subcarriers to different users for simultaneous transmission. OFDMA does not affect sensing performance as it does not influence the collected CSI at *SenCom*. As for the MU-MIMO, it is an extended version of the beamforming

mentioned above and the steering matrix is constructed for multi-user simultaneous transmission by sniffing the feedback of NDP. Therefore, the proposed CSI calibration method for beamforming can be easily extended to deal with the impact brought by MU-MIMO as well.

6.2 Sensing Performance

In this part, we measure the sensing performance of *SenCom*. We conduct two types of experiments to verify the effectiveness of the CSI calibration and incentive strategy, respectively. These experiments inspect both the quality and quantity of the CSI collected at *SenCom*.

6.2.1 Experiment Setup and Metric. **Experiment setup:** To test the performance of the CSI calibration, we collect the CSI samples during the coherence time and compare the calibrated CSI of $N_{STS} \geq 2$ with the collected CSI of $N_{STS} = 1$. To test the performance of the incentive strategy, we expose *SenCom* to the real WiFi communication environment and perform the incentive strategy. We adopt two baseline schemes for comparison: traditional WiFi sensing introduced in Section 2.1 (Active), and passive CSI collection without calibration and incentive (Passive). In theory, Active sensing can achieve the best sensing performance. Over 20,000 CSI samples are collected during the experimental evaluation. **Metrics:** For the CSI calibration, we adopt *dynamic time warping (DTW)* [57] to measure the *CSI difference* between the calibrated CSI of $N_{STS} \geq 2$ and the collected CSI of $N_{STS} = 1$. It seeks the temporal alignment that minimizes Euclidean distance between aligned series and the CSI difference is defined as the minimal Euclidean distance. A lower CSI difference indicates lower deviations between the measured CSI from different modes, i.e., better performance of CSI calibration. All CSI samples are normalized to eliminate the effect of variation of channel gain. For the incentive strategy, we adopt *fill rate* to quantify its performance, which is defined as the probability of meeting the required CSI sampling rate. It is calculated as the ratio of the number of tests that meet the such requirement to the number of all tests. The time window of each test is set to 0.3 s. Although the expected CSI sampling rate is 100 packets/s, the sensing requirement is set as 95 packets/s since there would be a loss of packets even in active sensing.

[6]https://files.miot-global.com/files/mini_wifi_router/Mi%20routerminiEN.pdf
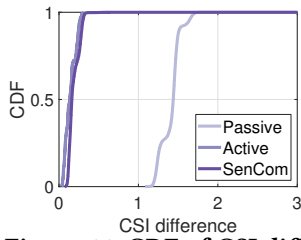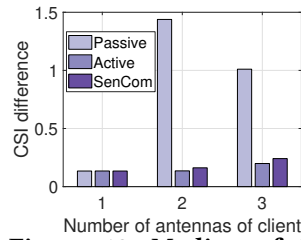
Figure 11: CDF of CSI difference.

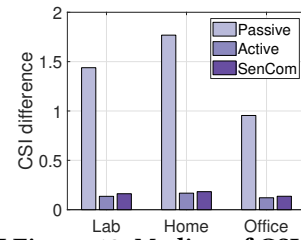**Figure 12: Median of CSI differences with different client's antenna numbers.**

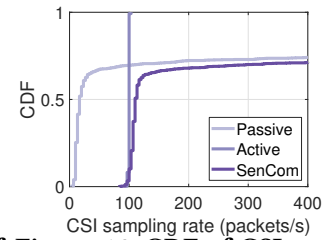**Figure 13: Median of CSI differences in three environments.**
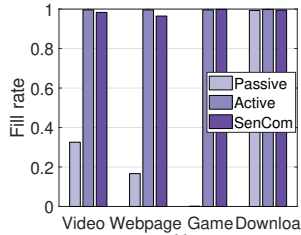

Figure 14: CDF of CSI sampling rate.
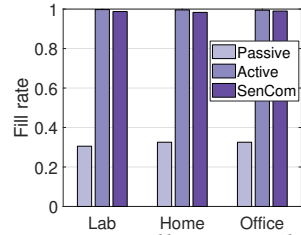

Figure 15: Fill rates with different communication tasks.

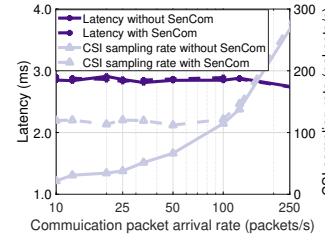**Figure 16: Fill rates in three communication environments.**

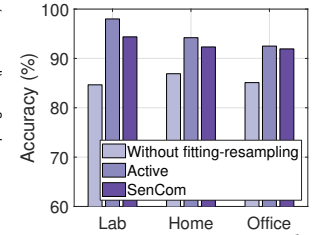**Figure 17: Communication performance.**

Figure 18: Accuracy in three environments.

Table 1: Communication performance with different communication tasks.

Task	Video	Webpage	Game		Download
Metric	Dropped rate	Loading time	Latency	Loss rate	Data rate
Without *SenCom*	1597/40477	614 ms	17 ms	0 %	88.68 Mbps
With *SenCom*	1613/40477	615 ms	17 ms	0 %	87.12 Mbps

6.2.2 Results. **Effectiveness of CSI calibration:** The cumulative distribution function (CDF) of the CSI difference for the three schemes is shown in Fig. 11. It can be seen that the CSI difference of Passive sensing is much higher than that of Active sensing, which indicates the low CSI quality issue due to the alternation of WiFi communication modes. By using the proposed CSI calibration method, the CSI difference of *SenCom* is greatly reduced to the level of Active sensing, without the need for active communication or coordination with the AP. Further, we show the median of the CSI difference with different client's antenna numbers in Fig. 12. The CSI difference of *SenCom* reaches that of Active sensing, which demonstrates that the CSI calibration can improve the quality of CSI. Besides, the CSI differences of the three schemes are almost the same when the antenna number is 1 because all packets are in the same communication mode. We also show the median of the CSI difference in three environments in Fig. 13. It can be found that the performance of the CSI calibration is not affected by the environment.
Effectiveness of incentive strategy: The CDF of CSI sampling rate is shown in Fig. 14. It can be found that the CSI sampling rate of Active sensing is stable, that is, about 100 packets/s all the time. On the contrary, when the client is playing an online video, the probability that the CSI sampling rate is higher than 100 packets/s is around 30% and

the CSI sampling rate is less than 40 packets/s in most cases, which cannot satisfy the sensing requirement at all times and may lead to the missing of key sensing information. It can be observed that the CSI sampling rate tends to exceed 100 packets/s with our proposed incentive strategy. In practical daily life, however, people may perform a variety of tasks on the Internet, such as visiting websites and playing online games. The fill rate for four communication tasks (namely video streaming, webpage surfing, online gaming, and download) are shown in Fig. 15. *SenCom* gives almost the same performance as that of Active sensing under different communication tasks, which demonstrates its effectiveness. The fill rate approaches 100% for the task of download as its communication demands are frequent and stable. Meanwhile, the medians of CSI sampling rate for the four communication tasks are 20.0 packets/s, 13.3 packets/s, 30.0 packets/s, and 503.3 packets/s, respectively. The corresponding intervals are 50.0 ms, 75.0 ms, 33.3 ms, and 2.0 ms, respectively. After applying the incentive strategy, the medians of CSI sampling rate for the four communication tasks are all higher than the sensing requirement. In addition, we also test the incentive strategy in three environments, as shown in Fig. 16. It can be seen that the fill rates are similar and near 100%. This indicates that the sensing requirement for sufficient CSI can

be satisfied in different environments with our incentive strategy.

6.3 Communication Performance

In this part, we measure the impact of *SenCom* on the normal WiFi communication performance.

6.3.1 Experiment Setup and Metric. **Experiment setup:** We test the communication performance in two ways. One is to directly measure the communication performance with the help of iperf[7] between the AP and client. The other is to measure the quality of experience (QoE) of the four aforementioned communication tasks. The communication performance is tested in a week randomly and the total time is more than 10 hours. Average results are shown in this part. **Metrics:** For the direct measurement, we adopt two metrics, i.e., *latency* and *throughput*, to quantify the communication performance. Latency describes the end-to-end delay between the AP and the client. Throughput is measured by the rate of successfully delivered data between the client and AP, which can be calculated as throughput = $\eta \lambda^c V$, where η is the successful delivery rate, λ^c is the packet arrival rate, and V is the data size per packet. For the task of webpage surfing, we utilize the *loading time* of the website to measure the QoE. For video streaming, its QoE is represented by the fluency of the video, i.e., *dropped rate* that is the number of dropped frames to the total number of frames. As for online gaming, we can use *latency* between the client and the game server and *loss rate* of operations. For the download task, its QoE is described by the data size delivered successfully per unit time, i.e., *data rate*.

6.3.2 Results. We evaluate the latency and throughput with different communication packet arrival rates. As shown in Fig. 17, the communication latency with *SenCom* is almost the same as that without *SenCom*. Especially, when the communication packet arrival rate is no less than the required CSI sampling rate, i.e., $\lambda^c \geq 100$ packets/s, there is no need to transmit incentive packets, and the latency thus is not affected at all. When $\lambda^c < 100$ packets/s, the loss can be reduced to a negligible level, i.e., less than 2%, by choosing a proper weight (i.e., $\beta = 0.1$). Meanwhile, according to the experiment results, the successful delivery rate without *SenCom* and with *SenCom* is 100%, indicating that *SenCom* does not affect the throughput. Fig. 17 also shows the average CSI sampling rate. With the incentive strategy, the CSI sampling rate is maintained constantly higher than required. By contrast, without the incentive strategy, the CSI sampling rate may fall short when the communication packet rate is low.

---

[7]https://iperf.fr/

The QoE of the four communication tasks is shown in Tab. 1. It can be observed that *SenCom* almost has no influence on the QoE of the communication tasks. Even for the download task that requires a very high data rate, the communication traffic is hardly impacted by the incentive strategy. Recalling that the required CSI sampling rate can be guaranteed according to the results in Fig. 15. Hence, with *SenCom* implemented in the communication system, sufficient CSI can be obtained for sensing without influencing ongoing communication traffic too much.

6.4 Case Study

We perform case studies to test *SenCom* with two real sensing applications: fall detection and step counting.

6.4.1 Experiment Setup and Metric. **Experiment setup:** We invite 15 volunteers (10 males and 5 females) aged from 19 to 29 to take part in the following two WiFi sensing applications: a classification application WiFall [73] and a measurement application WiStep [78]. WiFall is a learning-based fall detection system, which utilizes a random forest classifier to recognize four activities including walking, sitting down, standing up, and falling. WiStep is a modeling-based step counting system that can measure the number of steps with CSI samples. In each environment, five volunteers are requested to perform sensing experiments. The required CSI sampling rate is set to 100 packets/s. For each volunteer, we collect at least 200 training CSI samples and 150 testing CSI samples. We collect over 15,700 CSI samples for case studies. All experiments are conducted by adhering to the approval of our university's Institutional Review Board.
Metrics. We use *accuracy* [73] to quantify the classification performance for WiFall and *error rate* [78] to qualify the measurement performance for WiStep. Accuracy is measured by the percentage of correctly classified CSI samples, which is defined as $accuracy = \frac{N_{cor}}{N_{all}}$, where N_{cor} and N_{all} are the number of all correctly classified CSI samples and the number of all test samples, respectively. Error rate describes the difference between the estimated step count R_e and the ground truth value R_g, which is calculated by: $error\ rate = \frac{|R_e - R_g|}{R_g}$.

6.4.2 Results. **Overall performance.** We first derive the activity recognition accuracy when supporting WiFall in three environments. We compare *SenCom* with two schemes: simply collecting CSI without fitting-resampling, and Active sensing. The average accuracy of five persons in each environment is recorded. The accuracy of the three environments is shown in Fig. 18. It can be found that the accuracy of *SenCom* is higher than that without fitting-resampling. Thus, our fitting-resampling method can improve the activity recognition accuracy. The accuracy of *SenCom* is comparable to that of Active sensing, indicating that *SenCom* is qualified
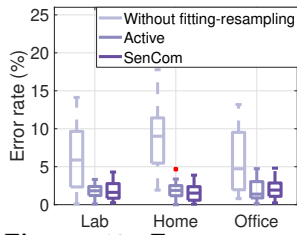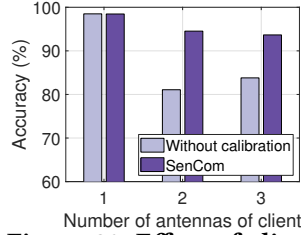
Figure 19: Error rates in three environments.

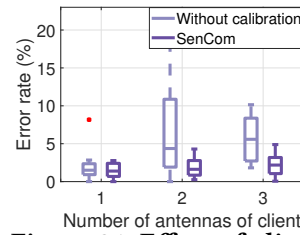**Figure 20: Effect of client's antenna number activity on accuracy.**

Figure 21: Effect of client's antenna number on error rate.
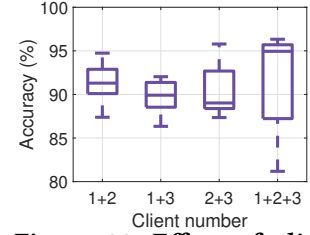

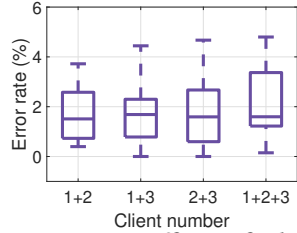**Figure 22: Effect of client number on accuracy.**

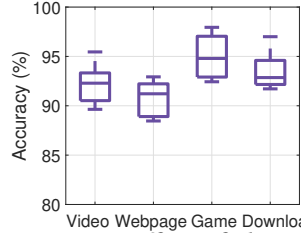**Figure 23: Effect of client number on error rate.**

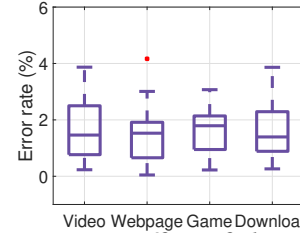**Figure 24: Effect of client activity on accuracy.**

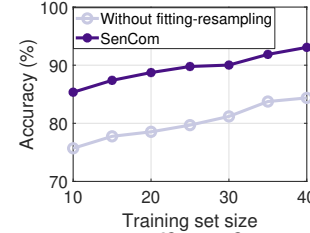**Figure 25: Effect of client activity on error rate.**

Figure 26: Effect of training set size on accuracy.

for classification tasks. Meanwhile, the accuracy of *SenCom* in lab, home, and office is 94.37%, 92.33%, and 91.93%, respectively. The accuracy is high and similar, demonstrating that *SenCom* performs well in different environments. The small accuracy differences are likely to be induced by random environmental noise. As for the step counting, we conduct comparison experiments similar to the activity recognition. The experimental results shown in Fig. 19 indicate that *SenCom*'s average error rates in lab, home, and office are 1.8%, 1.6%, and 2.0%, respectively. Meanwhile, it can be observed that our fitting-resampling method is also effective in measurement tasks. More importantly, the error rate of *SenCom* is comparable to that of Active sensing. The results suggest that *SenCom* can achieve outstanding performance in all WiFi-based sensing tasks, including both the classification and measurement ones.

Effect of client's antenna number: In this part, we use three clients equipped with one, two, and three antennas to explore the effect of the client's antenna number. To show the effectiveness of our CSI calibration method, we compare *SenCom* with an alternative: without CSI calibration. The experimental results of activity recognition and step counting are shown in Fig. 20 and Fig. 21, respectively. It can be seen that the performance when using one antenna is better than that of using two or three antennas. This is reasonable because *SenCom* does not need to execute CSI calibration when the client has only one receiving antenna. The CSI collected in this case is of higher quality. Meanwhile, the performance of *SenCom* is better than that of the alternative, which means that our CSI calibration method is very effective in improving the quality of CSI.

Effect of client number: In practice, multiple client devices may co-exist in the same WiFi domain. In this case, the transmitter is connected with multiple clients and transmits packets to different clients across time. To explore the effect of the client number, we conduct four experiments with four conditions. The experimental results of activity recognition and step counting are respectively displayed in Fig. 22 and Fig. 23, where '1 + 2' means that the transmitter is connected with a one-antenna client and a two-antenna client, and so forth. It can be observed that the performance of *SenCom* with different conditions is good and very similar to each other. This demonstrates the effectiveness of the CSI calibration, and as a result, the varied number of clients hardly affects the classification or measurement performance.

Effect of client activity: We also consider other communication traffic, i.e., online gaming, webpage surfing, and download. Figure 24 and Fig. 25 depict the activity recognition and step counting results when *SenCom* works with the above different communication traffic, respectively. As during download, the client has high communication demands, we disable the signal incentive. In Fig. 24, it can be found that online gaming can achieve the highest average accuracy. This is reasonable because online gaming does not initiate communication requests as frequently as other tasks. Most CSI is extracted from incentive packets that do not need to be calibrated, rendering better performance. But it is noteworthy that *SenCom* still performs well (93.53% accuracy and 1.65% error rate) under the worst conditions (i.e., download) where all the packets are from the communication traffic. This further demonstrates the effectiveness of our CSI calibration method.

Effect of training set size: Since WiFall adopts a learning-based method to achieve activity recognition, the size (i.e., the number of CSI samples) of the training set directly affects the activity recognition result. To explore if *SenCom* can still work well when the training set is small, we vary the number of the training CSI samples of each class from 10 to 40 and calculate the accuracy. Meanwhile, we compare *SenCom* with an alternative: without fitting-resampling. It can be observed from Fig. 26 that *SenCom* outperforms the alternative. When the number of CSI samples of each activity is 40, the accuracy reaches the highest. Nevertheless, the accuracy is still high (85%+) when only 10 CSI samples are collected for each class, which indicates that *SenCom* is insensitive to the training data size.

7 RELATED WORK

ISAC: Existing ISAC research mainly focuses on devising a special PHY design that is suitable for both communication and sensing. Most existing works require amendments to existing communication systems or protocols. There are two leading solutions: orthogonal resource allocation and unified waveform design [44]. In the former, sensing and communication systems share the same hardware. Orthogonal resources in temporal domain [27, 30, 41, 74], spectral domain [9, 65, 66], or spatial domain [20, 55] are allocated to two systems for reaching integration. Unlike them, unified waveform design [11, 28, 45, 46, 51] aims to design a dual-functional waveform, in which both wireless and hardware resources are shared. Compared with orthogonal resource allocation, spectrum efficiency can be improved. For instance, Liu *et al.* [45] optimize the trade-off between sensing and communications performance and design an optimal dual-functional waveform. Moreover, Chen *et al.* [13] propose a novel sensing framework, namely ISACoT, to achieve ISAC with encompassing time, frequency, space, and protocol aspects. Besides, there is a future WiFi standard on sensing, namely 802.11bf. It is an ongoing standard focusing on designing a new WLAN sensing procedure. Regardless of the sensing or communication performance, the above-mentioned designs require modifications to existing communication systems and are not compatible with most existing WiFi APs and devices. In this paper, we propose *SenCom* to achieve sensing without any modification to COTS WiFi systems. To our best knowledge, it is the first practical ISAC system that enables seamless WiFi sensing by sniffing communication traffic.

WiFi-based sensing: WiFi has been exploited for various sensing purposes. Existing WiFi-based sensing applications fall into two categories according to the sensing goals: detection/recognition and estimation [53]. Therein, detection and recognition are binary and multi-class classification tasks, respectively. The second category belongs to the measurement task. Detection systems usually aim at achieving binary sensing tasks, such as human presence detection [3, 22, 32, 59, 61, 62], fall detection [34, 60, 81], and motion detection [21, 25, 42, 49, 78, 79]. Recognition systems are generally utilized to accomplish multi-class prediction tasks, such as activity recognition [7, 17, 18, 37, 64], gesture recognition [2–5, 29, 36, 82], user identification [12, 14, 31, 47, 48, 70], and so on. In an estimation system, users can acquire quantitative feedback, such as location [33, 38, 40, 43, 56] and breathing rate [1, 50, 52, 71, 72]. Although a lot of previous works reuse WiFi frequency band and COTS WiFi devices to implement the sensing systems, none of them can directly work with normal WiFi 802.11ac/ax data traffic due to the impact of communication-oriented designs like MIMO and beamforming. In this paper, we design *SenCom* to enable sensing with such WiFi communication context. Particularly, the design of *SenCom* is independent of any specific sensing task. It helps an arbitrary sensing application in acquiring quality and sufficient CSI data without impairing ongoing normal WiFi communication.

8 CONCLUSION

In this paper, we propose *SenCom*, which enables WiFi sensing while maintaining communication capabilities. *SenCom* reuses the communication facilities and packets for sensing. In its design, we propose a CSI calibration method to obtain quality and unified CSI. Additionally, we introduce a fitting-resampling scheme to support upper-layer sensing applications with dimensionality-consistent CSI, and an incentive strategy that guarantees the sufficiency of CSI. The real-world experimental results demonstrate that *SenCom* is capable of supporting a variety of sensing applications, while retaining good communication performance.

REFERENCES

[1] Heba Abdelnasser, Khaled A. Harras, and Moustafa Youssef. 2015. UbiBreathe: A Ubiquitous non-Invasive WiFi-based Breathing Estimator. In *Proceedings of the ACM Symposium on Mobile Ad Hoc Networking and Computing (MobiHoc)*.

[2] Heba Abdelnasser, Moustafa Youssef, and Khaled A. Harras. 2015. WiGest: A ubiquitous WiFi-based gesture recognition system. In *Proceedings of the IEEE Conference on Computer Communications (INFOCOM)*.

[3] Fadel Adib and Dina Katabi. 2013. See through walls with WiFi!. In *Proceedings of the ACM Conference of the Special Interest Group on Data Communication (SIGCOMM)*.

[4] Kamran Ali, Alex X. Liu, Wei Wang, and Muhammad Shahzad. 2015. Keystroke Recognition Using WiFi Signals. In *Proceedings of the ACM Conference on Mobile Computing and Networking (MobiCom)*.

[5] Kamran Ali, Alex X. Liu, Wei Wang, and Muhammad Shahzad. 2017. Recognizing Keystrokes Using WiFi Devices. *IEEE Journal on Selected Areas in Communications (JSAC)* 35, 5 (2017), 1175–1190.

[6] IEEE Standards Association et al. 2016. IEEE Std 802.11-2016, IEEE standard for local and metropolitan area networks—part 11: Wireless LAN medium access control (MAC) and physical layer (PHY) specifications.

[7] Ibrahim Ethem Bagci, Utz Roedig, Ivan Martinovic, Matthias Schulz, and Matthias Hollick. 2015. Using Channel State Information for Tamper Detection in the Internet of Things. In *Proceedings of the ACM Computer Security Applications Conference (ACSAC)*.

[8] Boris Bellalta, Luciano Bononi, Raffaele Bruno, and Andreas Kassler. 2016. Next generation IEEE 802.11 Wireless Local Area Networks: Current status, future directions and open challenges. *Computer Communications* 75 (2016), 1–25.

[9] Marian Bică and Visa Koivunen. 2018. Radar waveform optimization for target parameter estimation in cooperative radar-communications systems. *IEEE Trans. Aerospace Electron. Systems* 55, 5 (2018), 2314–2326.

[10] Steven C Chapra and Raymond P Canale. 2013. Numerical Methods 6th Edition Chapra.

[11] Li Chen, Fan Liu, Weidong Wang, and Christos Masouros. 2021. Joint radar-communication transmission: A generalized pareto optimization framework. *IEEE Transactions on Signal Processing* 69 (2021), 2752–2765.

[12] Yuanying Chen, Wei Dong, Yi Gao, Xue Liu, and Tao Gu. 2017. Rapid: A Multimodal and Device-free Approach Using Noise Estimation for Robust Person Identification. *Proceedings of the ACM on Interactive, Mobile, Wearable and Ubiquitous Technologies (IMWUT)* 1, 3 (2017), 41:1–41:27.

[13] Zhe Chen, Tianyue Zheng, Chao Hu, Hangcheng Cao, Yanbing Yang, Hongbo Jiang, and Jun Luo. 2023. ISACoT: Integrating sensing with data traffic for ubiquitous IoT devices. *IEEE Communications Magazine* 61, 5 (2023), 98–104.

[14] Linsong Cheng and Jiliang Wang. 2016. How can I guard my AP?: non-intrusive user identification for mobile devices using WiFi signals. In *Proceedings of the ACM Symposium on Mobile Ad Hoc Networking and Computing (MobiHoc)*.

[15] IEEE Global Communications Conference. 2020. Workshop on Integrated Sensing and Communication. https://globecom2020.ieee-globecom.org/workshop/ws-05-workshop-integrated-sensing-and-communication-isac.

[16] Guangyao Ding, Jiantao Yuan, Jianrong Bao, and Guanding Yu. 2020. LSTM-Based Active User Number Estimation and Prediction for Cellular Systems. *IEEE Wireless Communications Letters* 9, 8 (2020), 1258–1262.

[17] Shihong Duan, Tianqing Yu, and Jie He. 2018. WiDriver: Driver Activity Recognition System Based on WiFi CSI. *International Journal of Wireless Information Networks* 25, 2 (2018), 146–156.

[18] Chunhai Feng, Sheheryar Ali Arshad, and Yonghe Liu. 2017. MAIS: Multiple Activity Identification System Using Channel State Information of WiFi Signals. In *Proceedings of the Wireless Algorithms, Systems, and Applications - International Conference (WASA)*.

[19] Victor S Frost and Benjamin Melamed. 1994. *IEEE Communications Magazine* 32, 3 (1994), 70–81.

[20] Rong Fu, Satish Mulleti, Tianyao Huang, Yimin Liu, and Yonina C Eldar. 2020. Hardware prototype demonstration of a cognitive radar with sparse array antennas. *Electronics Letters* 56, 22 (2020), 1210–1212.

[21] Liangyi Gong, Wu Yang, Dapeng Man, Guozhong Dong, Miao Yu, and Jiguang Lv. 2015. WiFi-Based Real-Time Calibration-Free Passive Human Motion Detection. *Sensors* 15, 12 (2015), 32213–32229.

[22] Liangyi Gong, Wu Yang, Zimu Zhou, Dapeng Man, Haibin Cai, Xiancun Zhou, and Zheng Yang. 2016. An adaptive wireless passive human detection via fine-grained physical layer information. *Ad Hoc Networks* 38 (2016), 38–50.

[23] Michael Grant and Stephen Boyd. 2014. CVX: Matlab software for disciplined convex programming, version 2.1.

[24] Francesco Gringoli, Matthias Schulz, Jakob Link, and Matthias Hollick. 2019. Free your CSI: A channel state information extraction platform for modern Wi-Fi chipsets. In *Proceedings of the Workshop on Wireless Network Testbeds, Experimental Evaluation & Characterization*.

[25] Yu Gu, Jinhai Zhan, Yusheng Ji, Jie Li, Fuji Ren, and Shangbing Gao. 2017. MoSense: An RF-Based Motion Detection System via Off-the-Shelf WiFi Devices. *IEEE Internet of Things Journal (IoTJ)* 4, 6 (2017), 2326–2341.

[26] Jerry R Hampton. 2013. *Introduction to MIMO communications*. Cambridge university press.

[27] Liang Han and Ke Wu. 2013. Joint wireless communication and radar sensing systems-state of the art and future prospects. *IET Microwaves, Antennas & Propagation* 7, 11 (2013), 876–885.

[28] Aboulnasr Hassanien, Moeness G Amin, Yimin D Zhang, and Fauzia Ahmad. 2015. Dual-function radar-communications: Information embedding using sidelobe control and waveform diversity. *IEEE Transactions on Signal Processing* 64, 8 (2015), 2168–2181.

[29] Wenfeng He, Kaishun Wu, Yongpan Zou, and Zhong Ming. 2015. WiG: WiFi-Based Gesture Recognition System. In *Proceedings of the IEEE Conference on Computer Communication and Networks (ICCCN)*.

[30] Yinghui He, Guanding Yu, Yunlong Cai, and Haiyan Luo. 2023. Integrated sensing, computation, and communication: system framework and performance optimization. *IEEE Transactions on Wireless Communications* (2023). https://doi.org/10.1109/TWC.2023.3285869

[31] Feng Hong, Xiang Wang, Yanni Yang, Yuan Zong, Yuliang Zhang, and Zhongwen Guo. 2016. WFID: Passive Device-free Human Identification Using WiFi Signal. In *Proceedings of the ACM Conference on Mobile and Ubiquitous Systems: Computing, Networking and Services (MobiQuitous)*.

[32] Jingzhi Hu, Tianyue Zheng, Zhe Chen, Hongbo Wang, and Jun Luo. 2023. MUSE-Fi: Contactless MUti-person SEnsing Exploiting Near-field Wi-Fi Channel Variation. In *Proceedings of the ACM Conference on Mobile Computing and Networking (MobiCom)*. 1–15.

[33] Nathaniel Husted and Steven A. Myers. 2010. Mobile location tracking in metro areas: malnets and others. In *Proceedings of the ACM Conference on Computer and Communications Security (CCS)*.

[34] Sijie Ji, Yaxiong Xie, and Mo Li. 2022. SiFall: Practical Online Fall Detection with RF Sensing. In *Proceedings of the ACM Conference on Embedded Networked Sensor Systems (SenSys)*.

[35] Chengkun Jiang, Junchen Guo, Yuan He, Meng Jin, Shuai Li, and Yunhao Liu. 2020. mmVib: micrometer-level vibration measurement

with mmwave radar. In *Proceedings of the ACM Conference on Mobile Computing and Networking (MobiCom)*.

[36] Dehao Jiang, Mingqi Li, and Chunling Xu. 2020. WiGAN: A WiFi Based Gesture Recognition System with GANs. *Sensors* 20, 17 (2020), 4757.

[37] Wenjun Jiang, Chenglin Miao, Fenglong Ma, Shuochao Yao, Yaqing Wang, Ye Yuan, Hongfei Xue, Chen Song, Xin Ma, Dimitrios Koutsonikolas, Wenyao Xu, and Lu Su. 2018. Towards Environment Independent Device Free Human Activity Recognition. In *Proceedings of the ACM Conference on Mobile Computing and Networking (MobiCom)*.

[38] Kiran Raj Joshi, Dinesh Bharadia, Manikanta Kotaru, and Sachin Katti. 2015. WiDeo: Fine-grained Device-free Motion Tracing using RF Backscatter. In *Proceedings of the USENIX Symposium on Networked Systems Design and Implementation (NSDI)*.

[39] Joonsuk Kim and Inkyu Lee. 2015. 802.11 WLAN: history and new enabling MIMO techniques for next generation standards. *IEEE Communications Magazine* 53, 3 (2015), 134–140.

[40] Minkyong Kim. 2013. Modeling Users' Mobility among WiFi Access Points. In *Proceedings of the USENIX International Workshop on Wireless Traffic Measurements and Modeling (WiTMeMo)*.

[41] Guoliang Li, Shuai Wang, Jie Li, Rui Wang, Fan Liu, Meihong Zhang, Xiaohui Peng, and Tony Xiao Han. 2021. Rethinking the Tradeoff in Integrated Sensing and Communication: Recognition Accuracy versus Communication Rate. *arXiv preprint arXiv:2107.09621* (2021).

[42] Shengjie Li, Xiang Li, Kai Niu, Hao Wang, Yue Zhang, and Daqing Zhang. 2017. AR-Alarm: An Adaptive and Robust Intrusion Detection System Leveraging CSI from Commodity Wi-Fi. In *Enhanced Quality of Life and Smart Living - International Conference (ICOST)*.

[43] Xiang Li, Daqing Zhang, Qin Lv, Jie Xiong, Shengjie Li, Yue Zhang, and Hong Mei. 2017. IndoTrack: Device-Free Indoor Human Tracking with Commodity Wi-Fi. *Proceedings of the ACM on Interactive, Mobile, Wearable and Ubiquitous Technologies (IMWUT)* 1, 3 (2017), 72:1–72:22.

[44] Fan Liu, Yuanhao Cui, Christos Masouros, Jie Xu, Tony Xiao Han, Yonina C Eldar, and Stefano Buzzi. 2021. Integrated sensing and communications: Towards dual-functional wireless networks for 6G and beyond. *arXiv preprint arXiv:2108.07165* (2021).

[45] Fan Liu, Christos Masouros, Ang Li, Huafei Sun, and Lajos Hanzo. 2018. MU-MIMO communications with MIMO radar: From co-existence to joint transmission. *IEEE Transactions on Wireless Communications (TWC)* 17, 4 (2018), 2755–2770.

[46] Fan Liu, Christos Masouros, Athina P Petropulu, Hugh Griffiths, and Lajos Hanzo. 2020. Joint radar and communication design: Applications, state-of-the-art, and the road ahead. *IEEE Transactions on Communications* 68, 6 (2020), 3834–3862.

[47] Hongbo Liu, Yan Wang, Jian Liu, Jie Yang, and Yingying Chen. 2014. Practical user authentication leveraging channel state information (CSI). In *Proceedings of the ACM Symposium on Information, Computer and Communications Security (ASIA CCS)*.

[48] Hongbo Liu, Yan Wang, Jian Liu, Jie Yang, Yingying Chen, and H. Vincent Poor. 2018. Authenticating Users Through Fine-Grained Channel Information. *IEEE Transactions on Mobile Computing (TMC)* 17, 2 (2018), 251–264.

[49] Jialin Liu, Lei Wang, Linlin Guo, Jian Fang, Bingxian Lu, and Wei Zhou. 2017. A research on CSI-based human motion detection in complex scenarios. In *Proceedings of the IEEE Conference on e-Health Networking, Applications and Services (Healthcom)*.

[50] Xuefeng Liu, Jiannong Cao, Shaojie Tang, Jiaqi Wen, and Peng Guo. 2016. Contactless Respiration Monitoring Via Off-the-Shelf WiFi Devices. *IEEE Transactions on Mobile Computing (TMC)* 15, 10 (2016), 2466–2479.

[51] Xiang Liu, Tianyao Huang, Nir Shlezinger, Yimin Liu, Jie Zhou, and Yonina C Eldar. 2020. Joint transmit beamforming for multiuser MIMO communications and MIMO radar. *IEEE Transactions on Signal Processing* 68 (2020), 3929–3944.

[52] Junyi Ma, Yuxiang Wang, Hao Wang, Yasha Wang, and Daqing Zhang. 2016. When can we detect human respiration with commodity wifi devices?. In *Proceedings of the ACM Joint Conference on Pervasive and Ubiquitous Computing (UbiComp)*.

[53] Yongsen Ma, Gang Zhou, and Shuangquan Wang. 2019. WiFi Sensing with Channel State Information: A Survey. *Comput. Surveys* 52, 3 (2019), 46:1–46:36.

[54] Yongsen Ma, Gang Zhou, Shuangquan Wang, Hongyang Zhao, and Woosub Jung. 2018. SignFi: Sign language recognition using WiFi. *Proceedings of the ACM on Interactive, Mobile, Wearable and Ubiquitous Technologies* 2, 1 (2018), 1–21.

[55] Jasmin A Mahal, Awais Khawar, Ahmed Abdelhadi, and T Charles Clancy. 2017. Spectral coexistence of MIMO radar and MIMO cellular system. *IEEE Trans. Aerospace Electron. Systems* 53, 2 (2017), 655–668.

[56] Saurabh Maheshwari and Anil Kumar Tiwari. 2015. Walking parameters estimation through channel state information preliminary results. In *Proceedings of the IEEE Conference on Signal Processing and Communication Systems (ICSPCS)*.

[57] Meinard Müller. 2007. Dynamic time warping. *Information retrieval for music and motion* (2007), 69–84.

[58] Long D Nguyen, Hoang Duong Tuan, Trung Q Duong, and H Vincent Poor. 2019. Multi-user regularized zero-forcing beamforming. *IEEE Transactions on Signal Processing* 67, 11 (2019), 2839–2853.

[59] Sameera Palipana, Piyush Agrawal, and Dirk Pesch. 2016. Channel State Information Based Human Presence Detection using Nonlinear Techniques. In *Proceedings of the ACM Conference on Systems for Energy-Efficient Built Environments*.

[60] Sameera Palipana, David Rojas, Piyush Agrawal, and Dirk Pesch. 2017. FallDeFi: Ubiquitous Fall Detection using Commodity Wi-Fi Devices. *Proceedings of the ACM on Interactive, Mobile, Wearable and Ubiquitous Technologies (IMWUT)* 1, 4 (2017), 155:1–155:25.

[61] Kun Qian, Chenshu Wu, Zheng Yang, Yunhao Liu, Fu-gui He, and Tianzhang Xing. 2018. Enabling Contactless Detection of Moving Humans with Dynamic Speeds Using CSI. *ACM Transactions on Embedded Computing Systems (TECS)* 17, 2 (2018), 52:1–52:18.

[62] Kun Qian, Chenshu Wu, Zheng Yang, Yunhao Liu, and Zimu Zhou. 2014. PADS: Passive detection of moving targets with dynamic speed using PHY layer information. In *Proceedings of the IEEE Conference on Parallel and Distributed Systems (ICPADS)*.

[63] Sheldon M Ross. 2014. *Introduction to probability models*. Academic press.

[64] Mauro De Sanctis, Ernestina Cianca, Simone Di Domenico, Daniele Provenziani, Giuseppe Bianchi, and Marina Ruggieri. 2015. WIBECAM: Device Free Human Activity Recognition Through WiFi Beacon-Enabled Camera. In *Proceedings of the ACM Workshop on Physical Analytics*.

[65] Chenguang Shi, Fei Wang, Sana Salous, and Jianjiang Zhou. 2019. Joint subcarrier assignment and power allocation strategy for integrated radar and communications system based on power minimization. *IEEE Sensors Journal* 19, 23 (2019), 11167–11179.

[66] Chenguang Shi, Fei Wang, Mathini Sellathurai, Jianjiang Zhou, and Sana Salous. 2017. Power minimization-based robust OFDM radar waveform design for radar and communication systems in coexistence. *IEEE Transactions on Signal Processing* 66, 5 (2017), 1316–1330.

[67] IEEE Communication Society. 2021. Integrated Sensing and Communication. https://www.comsoc.org/publications/journals/ieee-jsac/cfp/integrated-sensing-and-communication.

[68] David Tse and Pramod Viswanath. 2005. *Fundamentals of wireless communication*. Cambridge university press.

[69] Laurens Van der Maaten and Geoffrey Hinton. 2008. Visualizing data using t-SNE. *Journal of machine learning research* 9, 11 (2008), 2579–2605.

[70] Fei Wang, Jinsong Han, Feng Lin, and Kui Ren. 2019. WiPIN: Operation-Free Passive Person Identification Using Wi-Fi Signals. In *Proceedings of the IEEE Global Communications Conference (GLOBECOM)*.

[71] Pei Wang, Bin Guo, Tong Xin, Zhu Wang, and Zhiwen Yu. 2017. Tiny-Sense: Multi-user respiration detection using Wi-Fi CSI signals. In *Proceedings of the IEEE Conference on e-Health Networking, Applications and Services (Healthcom)*.

[72] Xuyu Wang, Chao Yang, and Shiwen Mao. 2017. TensorBeat: Tensor Decomposition for Monitoring Multi-Person Breathing Beats with Commodity WiFi. *CoRR* abs/1702.02046 (2017).

[73] Yuxi Wang, Kaishun Wu, and Lionel M. Ni. 2017. WiFall: Device-Free Fall Detection by Wireless Networks. *IEEE Transactions on Mobile Computing (TMC)* 16, 2 (2017), 581–594.

[74] Henk Wymeersch, Gonzalo Seco-Granados, Giuseppe Destino, Davide Dardari, and Fredrik Tufvesson. 2017. 5G mmWave positioning for vehicular networks. *IEEE Wireless Communications* 24, 6 (2017), 80–86.

[75] Yaxiong Xie, Zhenjiang Li, and Mo Li. 2015. Precise Power Delay Profiling with Commodity WiFi. In *Proceedings of the ACM Conference on Mobile Computing and Networking (MobiCom)*.

[76] Jie Xiong and Kyle Jamieson. 2013. Securearray: Improving wifi security with fine-grained physical-layer information. In *Proceedings of the ACM Conference on Mobile Computing and Networking (MobiCom)*.

[77] Weiye Xu, Jianwei Liu, Shimin Zhang, Yuanqing Zheng, Feng Lin, Jinsong Han, Fu Xiao, and Kui Ren. 2021. RFace: Anti-Spoofing Facial Authentication Using COTS RFID. In *Proceedings of the IEEE Conference on Computer Communications (INFOCOM)*.

[78] Yang Xu, Wei Yang, Jianxin Wang, Xing Zhou, Hong Li, and Liusheng Huang. 2017. WiStep: Device-free Step Counting with WiFi Signals. *Proceedings of the ACM on Interactive, Mobile, Wearable and Ubiquitous Technologies (IMWUT)* 1, 4 (2017), 172:1–172:23.

[79] Hao Yang, Licai Zhu, and Weipeng Lv. 2017. A HCI Motion Recognition System Based on Channel State Information with Fine Granularity. In *Proceedings of the Wireless Algorithms, Systems, and Applications - International Conference (WASA)*.

[80] Taesang Yoo and Andrea Goldsmith. 2005. Optimality of zero-forcing beamforming with multiuser diversity. In *Proceedings of the IEEE International Conference on Communications (ICC)*.

[81] Daqing Zhang, Hao Wang, Yasha Wang, and Junyi Ma. 2015. Anti-fall: A Non-intrusive and Real-Time Fall Detector Leveraging CSI from Commodity WiFi Devices. In *Proceedings of the Conference on Smart Homes and Health Telematics (ICOST)*.

[82] Yue Zheng, Yi Zhang, Kun Qian, Guidong Zhang, Yunhao Liu, Chenshu Wu, and Zheng Yang. 2019. Zero-Effort Cross-Domain Gesture Recognition with Wi-Fi. In *Proceedings of the ACM Conference on Mobile Systems, Applications, and Services (MobiSys)*.